Large drought-induced aboveground live biomass losses in southern Rocky Mountain aspen forests

CHO-YING HUANG* and WILLIAM R. L. ANDEREGG†‡

*Department of Geography, National Taiwan University, Taipei, 10617, Taiwan, †Department of Biology, Stanford University, Stanford, CA 94305, USA, ‡Department of Global Ecology, Carnegie Institution for Science, Stanford, CA 94305, USA

Abstract

Widespread drought-induced forest mortality has been documented across multiple tree species in North America in recent decades, but it is a poorly understood component in terrestrial carbon (C) budgets. Recent severe drought in concert with elevated temperature likely triggered widespread forest mortality of trembling aspen (*Populus tremuloides*), the most widely distributed tree species in North America. The impact on the regional C budgets and spatial pattern of this drought-induced tree mortality, which has been termed 'sudden aspen decline (SAD)', is not well known and could contribute to increased regional C emissions, an amplifying feedback to climate change. We conducted a regional assessment of drought-induced live aboveground biomass (AGB) loss from SAD across 915 km^2 of southwestern Colorado, USA, and investigated the influence of topography on the severity of mortality by combining field measures, remotely sensed nonphotosynthetically active vegetation and a digital elevation model. Mean [± standard deviation (SD)] remote sensing estimate of live AGB loss was 60.3 ± 37.3 Mg ha^{-1}, which was 30.7% of field measured AGB, totaling 2.7 Tg of potential C emissions from this dieback event. Aspen forest health could be generally categorized as healthy (0–30% field measured canopy dieback), intermediate (31–50%), and SAD (51–100%), with the remote sensing estimated mean (± SD) live AGB losses of 26.4 ± 15.1, 64.5 ± 9.2, and 108.5 ± 24.0 Mg ha^{-1}, respectively. There was a pronounced clustering pattern of SAD on south-facing slopes due to relatively drier and warmer conditions, but no apparent spatial gradient was found for elevation and slope. This study demonstrates the feasibility of utilizing remote sensing to assess the ramification of climate-induced forest mortality on ecosystems and suggests promising opportunities for systematic large-scale C dynamics monitoring of tree dieback, which would improve estimates of C budgets of North America with climate change.

Keywords: Landsat, *Populus tremuloides*, San Juan National Forest, spectral mixture analysis, sudden aspen decline (SAD), trembling aspen

Received 6 September 2011 and accepted 17 October 2011

Introduction

Recent, global increases in drought-induced tree mortality have been recognized as a potentially major source of carbon emissions, but this component of forest carbon (C) cycling is poorly understood (see review by Allen *et al.*, 2010). Records showed that, starting as early as the late 1990s, consecutive years of drought with elevated temperature, along with outbreaks of insects, have resulted in massive tree mortality across a range of forest types in western North America (Breshears *et al.*, 2005; van Mantgem *et al.*, 2009). These forest mortality events can have a major influence on the regional and continental C cycles. For instance, pine mortality across much of western Canada led to estimated C emissions equivalent to 75% of those contributed by Canada's wildfires during a several year

period (Kurz *et al.*, 2008). The intensity and spatial extent of the perturbation could also alter C budgets and influence energy partitioning and hydrological cycles for several decades following periods of high mortality (Breshears *et al.*, 2005; Allen *et al.*, 2010; Anderson *et al.*, 2011; Royer *et al.*, 2011). Thus, a large-scale monitoring technique for estimating landscape level changes in C storage associated with widespread tree mortality could greatly improve our understanding of the role of these events in regional C cycles and budgets.

Trembling aspen (*Populus tremuloides*) (hereafter 'aspen') is the most widely distributed tree species in North America, ranging from Alaska to Mexico, and one of the most massive known organisms in the world, reaching 6000 Mg (1 Mg = 10^6 g) in a single clone (Mitton & Grant, 1996). Long-term aspen decline may be influenced by multiple factors such as insect/pathogen load or fire suppression favoring later-successional species as opposed to earlier successional aspen trees,

Correspondence: C.-Y. Huang, tel. + 886 2 3366 3733, fax + 886 2 2362 2911, e-mail: choying@ntu.edu.tw

independent of drought impacts (Shepperd *et al.*, 2001; Strand *et al.*, 2009a). Increasing decline of the aspen populations was first noticed in Utah in late 1990s (Bartos & Campbell, 1998), and then, massive mortality events were reported a few years after in other southwestern states (Worrall *et al.*, 2010; Anderegg *et al.*, in press) and Canada (Michaelian *et al.*, 2011). This widespread dieback event of aspen forests in the western United States has been come to be called sudden aspen decline (SAD) (Worrall *et al.*, 2008) (see examples in Fig. 1).

Multiple lines of evidence suggest that SAD was induced by a recent 'global-change-type drought', a severe drought coupled with elevated temperatures. This evidence includes spatial patterns of mortality indicative of water stress, significantly higher moisture stress on sites experiencing dieback, simulation of SAD sites as being partially outside aspen's 'climate envelope', and experimental drought manipulations that triggered similar signals as SAD (Worrall *et al.*, 2008; Rehfeldt *et al.*, 2009; Worrall *et al.*, 2010; Anderegg *et al.*, in press). While the physiological mechanisms of how drought induced SAD are likely complicated and currently being studied, preliminary evidence suggests that drought-induced hydraulic failure may play an important role in mediating aspen mortality during drought (McDowell *et al.*, 2008; Anderegg *et al.*, in press). Drought is considered to have induced SAD, but changes in bark beetle, pathogen, and other pest dynamics could contribute to the die-off as well (Worrall *et al.*, 2010; Marchetti *et al.*, in press). Previous aerial surveys revealed that SAD was most severe in southwestern Colorado and may affect up to 17% of Colorado aspen forests (Worrall *et al.*, 2008, 2010). The spatial pattern of SAD is patchy (Fig. 1a) in this topographically complex mountainous region and not well understood. Mortality primarily affects mature ramets (aspen trees), but the lack of subsequent sprouting indicates a root system decline that has been verified through field observations. This apparent mortality of roots in aspen affected by SAD suggests that many of these stands might permanently disappear (Mitton & Grant, 1996). Surprisingly, the impacts of SAD on regional C budgets have been paid much less attention relative to other ecosystems with drought-induced forest mortality such as pinyon-juniper woodlands (Breshears *et al.*, 2005; Shaw *et al.*, 2005) and pine forests (Kurz *et al.*, 2008; van Mantgem *et al.*, 2009).

It is challenging to estimate drought-induced live aboveground biomass (AGB) losses (defined as converting live trees to dead materials such as standing coarse woody debris, attached senescent leaves, and
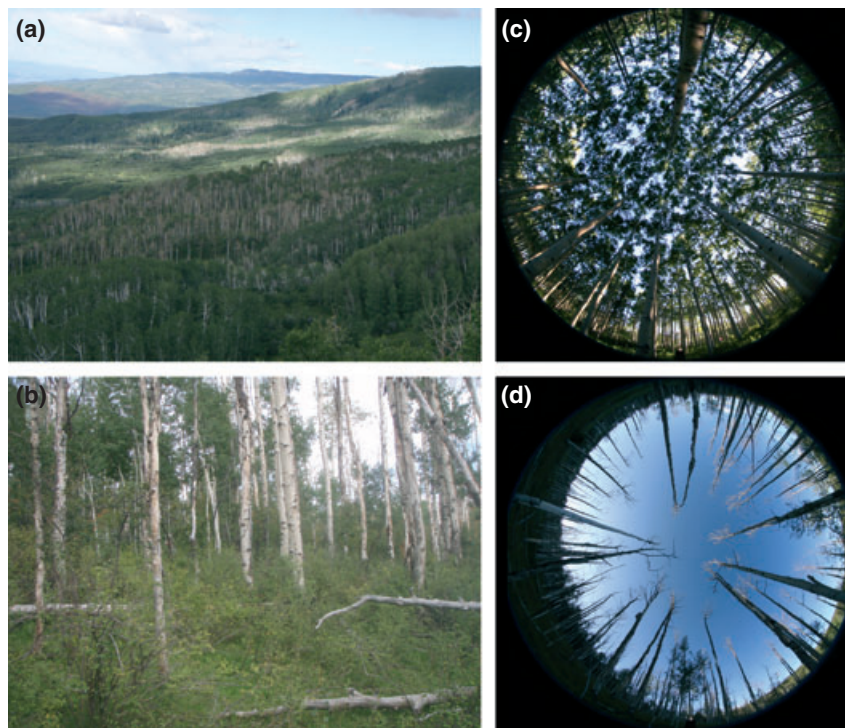

Fig. 1 (a) Landscape of sudden aspen decline (SAD) in the San Juan National Forest, Colorado, USA, and (b) dense mountain snowberry understory vegetation. The fisheye views indicate gap fractions of (c) a healthy aspen stand and (d) a SAD site. Photographs were taken by W. Anderegg in July 2010.

litter fall) across large forested regions. Previous studies have generally set up extensive field plots and manually estimated dead AGB by measuring stem diameters and/or height depending on the tree structures (Floyd *et al.*, 2009; Michaelian *et al.*, 2011). Although this approach is valid, the inevitable downside of such field surveys is the high cost of budget, manpower, and time, which hinders effective and repeated regional assessment. In addition, a substantial amount of aspen forests are distributed in remote mountainous regions (e.g., the Rocky Mountains), which would make frequent monitoring infeasible. Remote sensing provides a promising alternate approach. Strand *et al.* (2009b) utilized a spectral mixture analysis to compute fractional photosynthetic vegetation cover (PV) of aspen in mixed aspen-conifer vegetation from a fine spatial resolution, multispectral Landsat ETM+ (Enhanced Thematic Mapper plus) satellite image. Huang *et al.* (2010) demonstrated that losses of live AGB in pinyon-juniper woodlands can be estimated using time series of dry season PV derived from both Landsat Thematic Mapper (TM) and ETM+ images also by spectral mixture analysis (Asner & Heidebrecht, 2002). Assumptions were made that presummer monsoon PV in drylands can be used as a surrogate of woody cover since the majority of herbaceous plants (grasses, sedges, and forbs) are senescent during this driest time period (Breshears *et al.*, 2005; Huang *et al.*, 2007), and woody cover is a significant variable for predicting AGB at the Landsat scale (30 m) (Asner *et al.*, 2003; Huang *et al.*, 2009). PV is generally stable through time, and a rapid decline of PV may indicate the occurrence of tree dieback which can be used to estimate the losses of live AGB.

Such analysis, however, may require several cloud-free Landsat images through years which could be difficult in mountainous areas where clouds frequently accumulate due to orographic effects (Daly *et al.*, 1994). In addition, this approach may not be suitable for aspen or alpine forests since the loss of PV can be compensated by the green background of understory species such as mountain snowberry (*Symphoricarpos oreophilus*) from the satellite view (Fig. 1b), as opposed to the bare or low vegetation below the canopy of pinyon-juniper woodlands. Phenology of aspen and mountain snowberry is quite similar with leaf-out in late May, growth during the summer, and leaf-drop in late October. Therefore, the most promising variable that could be directly linked to SAD-induced live AGB loss is projected nonphotosynthetically active vegetation (NPV) cover, which can be computed using spectral mixture analysis (Chambers *et al.*, 2007). The relationship between NPV and biomass loss would then allow a large-scale assessment of the impacts of SAD on C budgets. In this study, we investigated the following questions: (a) What are the ramifications of SAD on the regional live C stocks in aspen forests? (b) Does terrain complexity amplify spatial heterogeneity of tree mortality? (c) Can remote sensing be an effective tool for regional estimation of SAD-induced live C loss?

Methods

Study site

We focused on aspen forests in the San Juan National Forest (SJNF), located in southwestern Colorado, USA, defined by Lowry *et al.* (2007). To match with the remote sensing analysis, we selected only the region covered by the Worldwide Reference System (WRS)-Path (P) 35 Row (R) 34, comprising about 915 km^2 (Fig. 2). The San Juan Mountains experience a summer rainy season that usually begins in July due to an influx of monsoonal air from the Gulf of Mexico and the Gulf of California. Winter storms typically cover higher elevations in snow in mid-November and generally cease in early May (Keen, 1996). Previous studies suggested a mean annual temperature of 3.2 °C and an average annual precipitation of 508 mm at high elevation weather stations (2660–2710 m), though this varies considerably across elevation (Elliot & Baker, 2004). Aspen forests are found in this region between elevations of ~2350–3250 m elevation, co-occurring with ponderosa pine (*Pinus ponderosa*) forests at the lower end and Engelmann spruce (*Picea engelmannii*)/subalpine fir (*Abies lasiocarpa*) forests at the upper end (Worrall *et al.*, 2008) (Fig. 2). Dominant understory species is the mountain snowberry (Fig. 1b).

Field observations

Surveys to assess stand biomass losses were conducted during June–August of 2009–2011. A total of 60 plots within stands were randomly located and measured with a Global Positioning System (Garmin eTrex Vista, Garmin International, Inc., Olathe, KS, USA) (Fig. 2a). We ensured that plots were not located within the same aspen clone by observing patterns and timing of leaf flush during late spring, as clonal boundaries can generally be determined based on timing of leaf flush. We measured diameter at breast height [DBH (cm)] and assessed percentage of canopy dieback (%) visually for all trees within one or four 6.3–8 m radius circles (0.012–0.05 ha), and snags and a few other tree species within the plots were excluded. Canopy dieback is defined as abnormal and recent senescence of branches and twigs within the tree crown at the stand level. Percent canopy dieback was assessed consistently across plots by two observers, which has been used successfully in other aspen mortality studies, and correlates well with changes in canopy area assessed with fish-eye photography (e.g., Worrall *et al.*, 2010; Anderegg *et al.*, in press). Due to the broad spatial extent of our study site, a generalized aspen allometry (Pastor *et al.*, 1984; Eqn 1) covering a wide range of
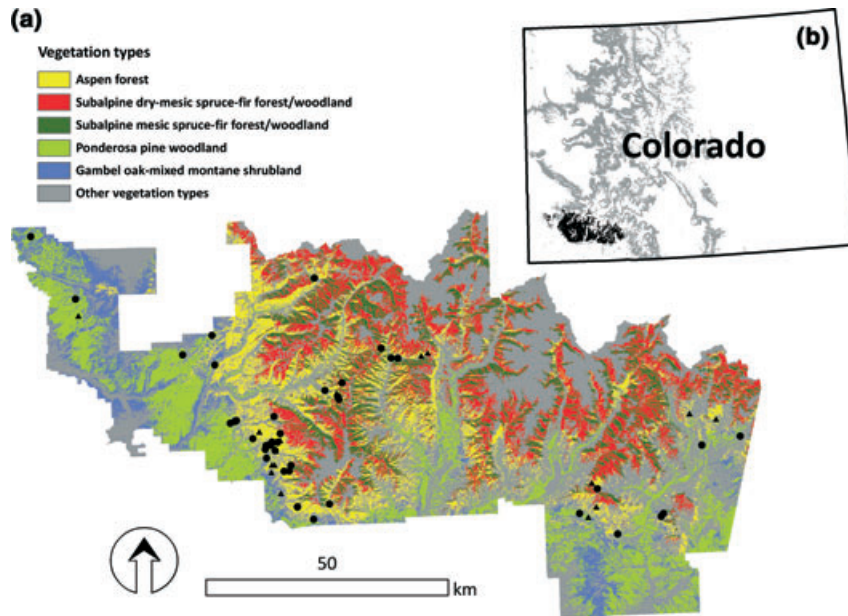
Fig. 2 (a) Major vegetation types in the San Juan National Forest, Colorado, USA, within the spatial coverage of Landsat World Reference System Path 35-Row 34. Areas labeled as 'other' are vegetation types too small to be depicted as separate colors mainly occupied by montane dry-mesic mixed conifer forest/woodland, aspen-mixed conifer forest/woodland, complex, montane mesic mixed conifer forest/woodland, dry tundra, and alpine bedrock/scree (Lowry *et al.*, 2007). Black circles (n = 42) and triangles (n = 18) are randomly assigned groups for the generation of the aspen live aboveground biomass loss model and estimation validation, respectively. (b) The location of study site (dark-colored pixels) and spatial extent of aspen vegetation (light-colored pixels) in Colorado.

tree sizes (DBH = 1.0–39.6 cm, n = 183) was utilized to estimate AGB for each individual ramet.

$$\ln{(\text{AGB[g]})} = 4.4564 + 2.4486\ln{(\text{DBH[cm]})}, R^2 = 0.992 \quad (1)$$

We tested the legitimacy of using a general model by comparing it with the region-specific allometrics and found a minor relative error of 4% of the mean value predicted by the generalized regression (Pastor *et al.*, 1984). We predicted percent live AGB loss per tree by multiplying biomass by percent canopy dieback since Gower *et al.* (1997) found a significant positive relationship between leaf area and DBH in aspen forests (Eqn 1). Loss of live biomass density (Mg ha^{-1}) of each plot was estimated by taking the plot sizes into account.

Remote sensing preprocessing

A cloud-free WRS-P35R34 2011 summer (July 1) Landsat TM image covering the study site was acquired from the US Geological Survey (USGS) Global Visualization Viewer (http://glovis.usgs.gov/). Landsat TM is a multispectral space-borne sensor containing six visible, near-infrared and shortwave infrared bands with a nominal spatial resolution of 30 m and one thermal band. Image preprocessing entailed radiometric calibration, including geometric registration and removal of atmospheric effects. The image was geo-registered by USGS prior to the acquisition in the Universal Transverse Mercator zone 12 N and the datum of the World Geodetic System 1984 (UTM zone 12 N, WGS 84). For atmospheric correction, the image was converted from raw digital count (8 bit) to surface reflectance (unitless, ranging from 0 to 1) using ACORN version 6 (ImSpec LLC, Palmdale, CA, USA). Only two atmospheric parameters are required for the multispectral mode: atmospheric water vapor and atmosphere visibility, and they were set to 15 mm and 100 km, respectively (ACORN, 2008).

Spectral mixture analysis

Spectral mixture analysis is a technique to derive subpixel cover fractions of surface materials collected from remotely sensed data (Adams *et al.*, 1993). In a natural setting, the main surface components (also known as endmembers) are PV, NPV, and bare soil. The method is ideal for use in these heterogeneous settings where subpixel cover variation is high. Each endmember component contributes to the pixel-level spectral reflectance (ρ_{pixel}) as the linear combination of endmember (e) spectra:

$$\rho_{\text{pixel}} = \Sigma[\rho_e \cdot C_e] + \varepsilon$$
$$= [\rho_{\text{PV}} \cdot C_{\text{PV}} + \rho_{\text{NPV}} \cdot C_{\text{NPV}} + \rho_{\text{soil}} \cdot C_{\text{soil}}] + \varepsilon \quad (2)$$

$$\Sigma[C_e] = 1.0, \quad (3)$$

where C is the cover fraction of each endmember (PV, NPV, and bare soil) and ε is the error term (Eqn 2). Equation (3) indicates that the endmembers sum to unity. Asner *et al.* (2000) found that there were a number of endmember combinations that can produce a particular spectral signal, so a wide range of numerically acceptable unmixing results for any image
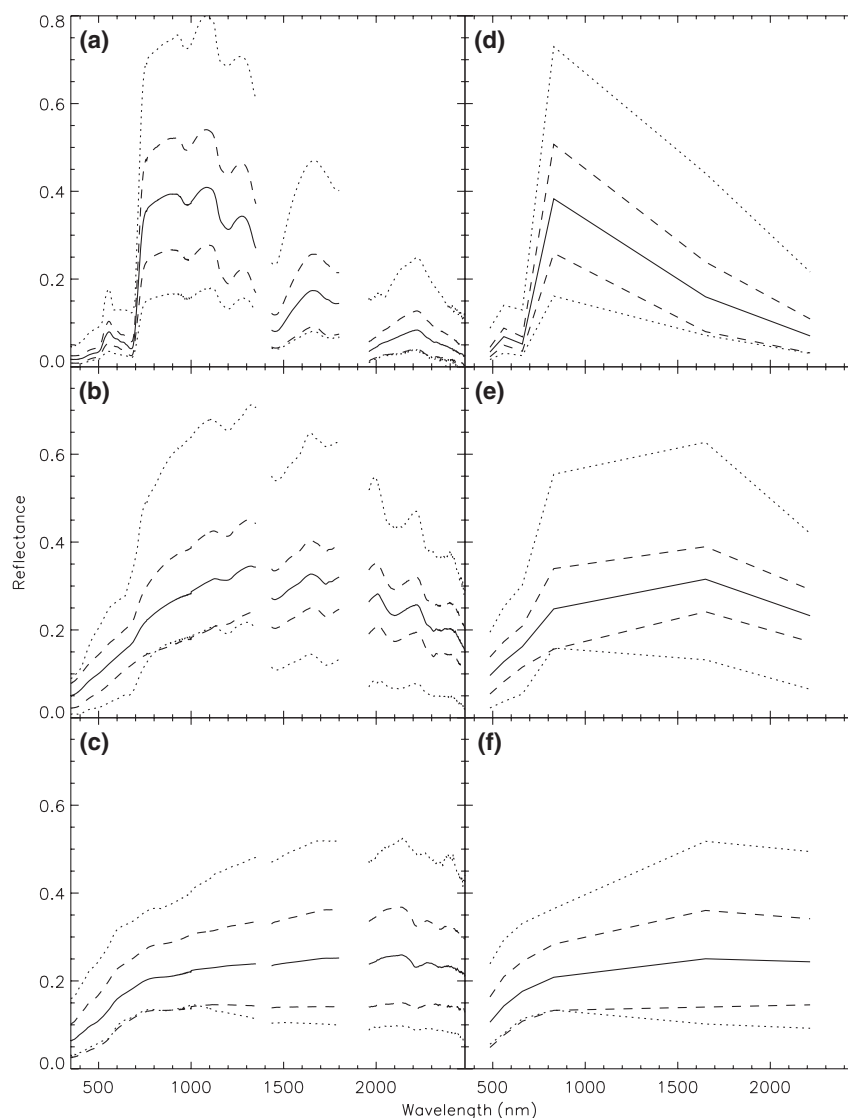
Fig. 3 Endmember reflectance bundles of (a) photosynthetically active vegetation (PV), (b) nonphotosynthetically active vegetation (NPV), and (c) bare soil collected from a field portable spectroradiometer, and these endmember reflectance bundles were re-sampled to match the spectral intervals of Landsat Thematic Mapper (TM) bands [(d) PV, (e) NPV, and (f) bare soil] to spectrally unmix the 2011 summer Landsat TM image. Solid lines indicate mean values; dashed lines indicate one standard deviation on each side of mean, and dotted lines are minimum and maximum reflectance values.

pixel were possible. Hence, an advanced spectral mixture analysis technique, known as Automated Monte Carlo Unmixing (AutoMCU), was implemented to account for this natural variability (Asner & Lobell, 2000) through iterative random selection of endmember reflectance from 'bundles' (Bateson et al., 2000). We acquired endmember bundles for PV (n = 83), NPV (n = 51), and bare soil (n = 40) collected from similar bio-climatic regions from the National Biological Information Infrastructure (http://frames.nbii.gov), US Geological Survey Digital Spectral Library (http://speclab.cr.usgs.gov), and Drought Impacts on Regional Ecosystems Network (http://www4.nau.edu/direnet/index.html). These spectral data were collected from fields by a full optical range (350–2500 nm), 1 nm resolution spectroradiometer (Fig. 3a–c), and

were convoluted to six broad spectral bands to match up with the TM spectral profiles (Fig. 3d–f). For each pixel, 250 independent, iterative unmixing procedures (Eqn 2) were applied to extract the most probable fractional cover of PV, NPV, and bare soil.

Regional estimation of SAD-induced live AGB loss

A regression model was utilized using 70% (n = 42) randomly selected field observed live AGB loss plots as the dependent variable and spatially corresponding NPV faction as the independent variable. The spatial independence was investigated using Moran's *I* using ArcGIS version 9.3 spatial statistics tools (ESRI, Redlands, CA, USA). It is a weighted correlation
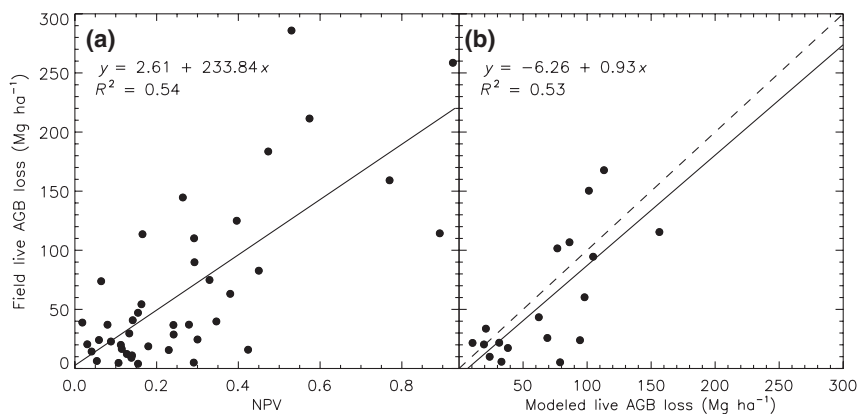
Fig. 4 (a) The regression model ($n = 42$) using fractional cover of nonphotosynthetically active vegetation (NPV) as an independent variable to estimate aspen live aboveground biomass (AGB) losses (Mg ha^{-1}). (b) Relationship between field estimated ($n = 18$) and modeled AGB using (a). The dashed line depicts 1 : 1 relationship, and the solid line shows correlation relationship.

coefficient for assessing the randomness of a spatial data pattern (Moran, 1950). The index has been commonly used in sampling designs for environmental studies (Fortin *et al.*, 1989). The range of Moran's *I* in most cases is from −1 (highly diffuse) to +1 (highly clustered). If the value for a Moran's *I* statistic for lacking spatial autocorrelation is close to 0, this indicates a standard statistical analysis can be directly applied (Fortin & Dale, 2005). The remaining 30% of samples ($n = 18$) were used for model validation. The absolute difference and the slope/offset of correction between the model prediction and ground truth were referred as indices to evaluate the performance of model (e.g., slope close to 1 with low offset constitutes reasonable performance). Based on the correlation between NPV and field estimated aspen live AGB loss, we can map the impact of SAD on aspen AGB in SJNF. To further validate the result, we visually compared our regional live AGB loss continuous estimates with another independent set of nominal (high mortality, low mortality) tree mortality data generated by locating forest mortality patches from an aircraft and delineating them manually onto a Geographic Information System (GIS) base map by 2010 USFS Forest Health Aerial Survey (for details: http://csfs.colostate.edu/pages/common-insects.html).

Aspen forest health status and topographical analysis

With the availability of regional estimates of aspen live AGB loss, we sought to investigate the influence of topography to aspen mortality. To facilitate the analysis, we partitioned the aspen mortality gradient into three general groups: healthy,

intermediate, and SAD by referring to the proportion (%) of field samples and live AGB loss within each canopy dieback interval (0–10%, 10–20%, ⋯ 90–100%). In additional, we regressed percent canopy dieback with live AGB loss. Coupling this correlation and the regional estimates of aspen, AGB loss permits regional mapping of spatial patterns of aspen mortality classes. Relationships between live AGB loss and topography were analyzed by integrating the mortality classes and a 30 m digital elevation model (DEM), which was originally used to ortho-rectify the TM image. Thus, the geo-registrations for the live AGB loss data and DEM were seamlessly matched. The DEM-derived slope and aspect were computed using ArcGIS. Aspect was originally in degrees (°), but was grouped into six nominal classes: north (N: 0–30° and 330–360°), northeast (NE: 31–90°), southeast (SE: 91–150°), south (S: 151–210°), southwest (SW: 211–270°), and northwest (NW: 271–330°). Additionally, flat terrain without apparent facing was excluded from this analysis. The topographical characteristics of each mortality group (healthy, intermediate, SAD) were extracted, weighted (for aspect only), and compared.

Results

Field observations

Mean density (± SD) of the randomly selected plots ($n = 60$) was 1104.1 ± 551.5 ramets ha^{-1} ranging from 481.2 to 3133.4 ramets ha^{-1} with mean DBH (± SD) of 22.4 ± 5.6 cm (range = 10.7–39.1 cm). Based on the DBH measures and allometry (Eqn 1), we computed the mean

Table 1 Characteristics of health statuses of aspen forests in the San Juan National Forest, Colorado, USA. The abbreviation of AGB, SAD, and SD are aboveground biomass, sudden aspen decline, and standard deviation, respectively

Category	Percent canopy dieback (%)	Percent area (%)	Live AGB loss range (Mg ha^{-1})	Mean live AGB loss ± SD (Mg ha^{-1})
Healthy	0–30	42.1	0–49.1	26.4 ± 15.1
Intermediate	31–50	31.0	49.1–81.4	64.5 ± 9.2
SAD	51–100	26.9	81.4–236.4	108.5 ± 24.0

($\pm$ SD) AGB of each plot in the aspen forests of 196.3 $\pm$ 94.3 Mg ha^{-1}. Our field observations revealed 30% of plots experienced significant canopy dieback (>50%) and the mean ($\pm$ SD) level of dieback was 35.0 $\pm$ 31.0%. Coupling proportion of canopy dieback with AGB estimates, we determined mean ($\pm$ SD) field aspen live AGB losses were 62.5 $\pm$ 64.7 Mg ha^{-1} ranging from 4.0 to 285.9 Mg ha^{-1}.

Remote sensing estimates

Moran's *I* values for field live AGB loss and remote sensing NPV observations were -0.01 (z-score = 0.50, $P = 0.61$) and -0.03 (z-score = -0.34, $P = 0.73$), respectively, which suggested relatively little clustering of field sites and permitted the use of a standard statistical model. A significant linear relationship ($R^2 = 0.54$, $P < 0.0001$, $n = 42$) was found between field estimated live AGB losses and remote sensing NPV cover fractions (Fig. 4a). Mean difference ($\pm$ SD) between the model prediction (Fig. 4b) and field observation was moderate (30.0 $\pm$ 21.4 Mg ha^{-1}), and the statistical relationship between these modeled and true values was linear and positive ($R^2 = 0.53$, $P = 0.0007$) (Fig. 4b). In addition, the slope of regression line is very close to the 1 : 1 relationship with a minor offset (-6.3 Mg ha^{-1}). Therefore, the validation results suggest the use of the model is reasonable and relatively robust.

By integrating the live AGB loss-NPV fraction model (Fig. 4a) and fractional cover of NPV derived from the summer 2011 Landsat TM image, we were able to estimate aspen live AGB losses at the landscape scale (Fig. 5a). There is a strong agreement between our continuous AGB loss estimate and 2010 US Forest Service aerial tree mortality mapping based on the visual assessment (Fig. 5). According to the analysis, the aspen forests experienced different degrees of live AGB losses ranging from 8.6 to 236.4 Mg ha^{-1}, though areas with low levels of AGB loss may occur due to background rates of branch/ramet mortality rather than drought-induced dieback. Mean ($\pm$ SD) live AGB loss for the study region was 60.3 $\pm$ 37.3 Mg ha^{-1}. After taking the size of aspen forests in the region (915 km^2) and the species specific biomass-C conversion coefficient of 0.492 (Kaakinen *et al.*, 2004) into account, we estimated the total live C losses (potential C emissions) in aspen forests of the region were 2.7 Tg C (1 Tg = 10^{12} g).

Aspen health status and topographical analysis

Three distinct tree mortality groups [healthy (0–30%, $n = 38$), intermediate (31–50%, $n = 4$), SAD (51–100%, $n = 18$)] were observed by investigating the profile of field collected canopy dieback gradient and their corre-
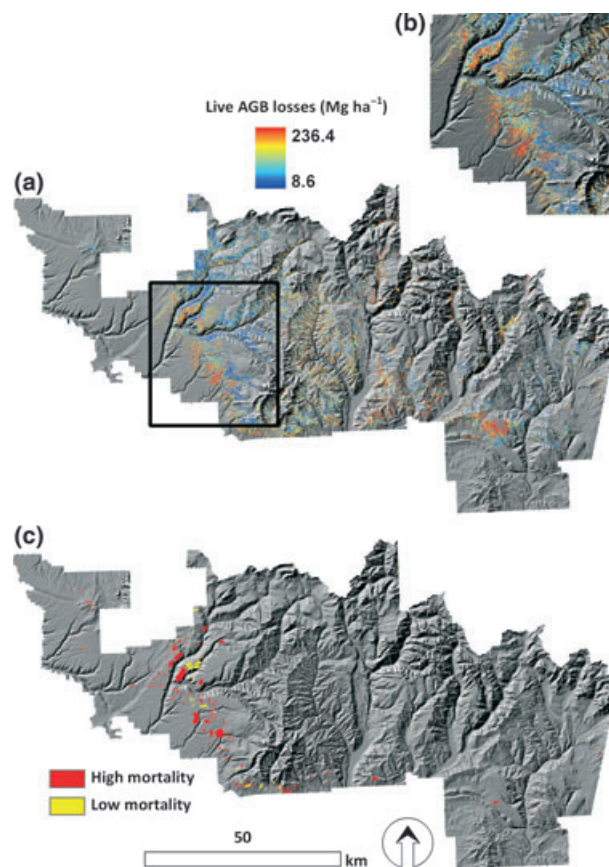

Fig. 5 (a) Regional continuous estimates of live aspen aboveground biomass (AGB) losses of aspen in the San Juan National Forest, Colorado, USA. The background is a hillshaded digital elevation model. (b) A close-up look of live AGB losses in a severely damaged area. (c) Nominal mortality classes produced by the 2010 USFS Forest Health Aerial Survey.

sponding live AGB losses (Fig. 6a). In addition, a significant log-log (which appears linear-like) relationship ($R^2 = 0.78$, $P < 0.0001$) was found between field live AGB loss and canopy dieback (Fig. 6b). Combining the aforementioned information and remote sensing aspen live AGB loss map allowed us to assess the health status of aspen forest in the SJNF (Table 1). Results show that 57.9% of aspen forests have been impacted by the recent tree mortality events (Intermediate and SAD categories), and mean live AGB loss of these severely damaged areas (canopy dieback > 50%) is 55.3% of the field estimated mean AGB.

By integrating the spatial layers of live AGB losses (Fig. 5a), tree mortality groups (Fig. 6 and Table 1), and a DEM, we found that mean elevation and slope ranges are very similar among three groups, although the variation of elevation in SAD sites was greater than in the other two groups (Table 2). The proportions of slope facings for each group were weighted by the proportions
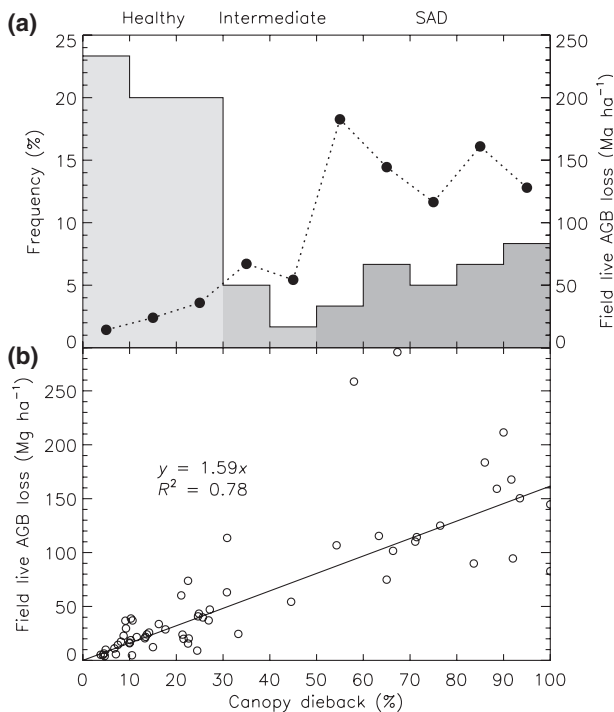
Fig. 6 (a) Frequencies (bars, total frequency = 100%) of field aspen canopy dieback observations (the left y-axis), and colors from light to dark indicating the severity of tree mortality based on the field plot measurement ($n = 60$). Black dots (the secondary y-axis) depict mean live aboveground biomass (AGB) losses of each interval. (b) The relationship between field observed live AGB losses of aspen and percent canopy dieback.

of population (N: 4.7%, NE: 10.2%, SE: 21.2%, S: 27.9%, SW: 24.8%, NW: 11.2%). The general trend depicts that impacted forests (intermediate and SAD groups) were most commonly found (mean = 20.8%) on the south and southeast facing slopes and less commonly found (14.0%) on the north-facing slopes.

Discussion

As the most widespread tree species on the continent, aspen forests play a role in the C budgets of both North American temperate and boreal forest ecosystems (Perala, 1990). In the Boreal Ecosystem-Atmosphere Study (BOREAS) sites in Canada, boreal aspen forests contained the highest forest biomass of all measured species with an estimated 153.6 Mg ha^{-1} of living AGB (Gower et al., 1997). Boreal aspen forests consistently exhibited the highest annual aboveground net primary productivity and are considered to be strong C sinks, though this can vary greatly with drought stress (Gower et al., 1997; Barr et al., 2007). Recent drought-induced aspen dieback in that region led to a conservatively estimated 14 Tg C potentially emitted from these boreal aspen forests, equivalent to about 7% of Canada's actual anthropogenic C emissions (Michaelian et al., 2011). Aspen forests figure prominently in temperate forest C budgets as well, as they comprise substantial portions of forest ecosystems in the Rocky Mountains, Great Lakes states, and eastern deciduous forests (Perala,

Table 2 Mean topographical characteristics (± standard deviation) of aspen forests experiencing different levels of canopy dieback (see Table 1 for details) in the study region, derived from a digital elevation model. The proportion of aspect classes [N: north ($n = 47\ 097$), NE: northeast ($n = 102\ 970$), SE: southeast ($n = 213\ 520$), S: south ($n = 281\ 101$), SW: southwest ($n = 249\ 846$), NW: northwest (113 345)] is weighted by their proportion to the population

Category	Elevation (m)	Slope (°)	Aspect N/NE/SE/S/SW/NW (%)
Healthy	2848.6 ± 184.8	17.8 ± 9.7	22.6/16.2/11.4/12.5/16.9/20.6
Intermediate	2849.7 ± 202.5	19.1 ± 10.7	13.1/17.7/19.8/19.2/16.4/13.8
SAD	2869.4 ± 211.3	17.7 ± 11.4	9.6/16.4/23.1/21.7/16.6/12.6

Table 3 Summary of studies estimating drought-induced mean live aboveground biomass losses in North America. Areas for the spatial analysis studies are the modeled land areas using remote sensing (Huang et al., 2010, and this study) or spatial statistics (Michaelian et al., 2011), and those for the field survey literature refer to ground sampled plots

Approach	Species	Region	Mean loss (Mg ha^{-1})	Area (ha)	Reference
Spatial analysis	Aspen	Southwest Colorado	60.3	9.15×10^4	This study
	Aspen	Central Canada	20.0	2.27×10^6	Michaelian et al. (2011)
	Pinyon pine	Southwest Colorado	20.0	4.10×10^5	Huang et al. (2010)
Field survey	Aspen	Southwest Colorado	67.2	2.34	Anderegg et al. (in press)
	Lodgepole pine	Central Idaho	37.8	0.48	Pfeifer et al. (2011)
	Pinyon pine	Southwest Colorado	24.0	3.24	Floyd et al. (2009)

1990; Curtis *et al.*, 2002). Our estimate of 2.7 Tg of potential C emissions from live AGB loss from this region alone is equivalent to 36.5% of Colorado's annual residential emissions or 6.8% of Colorado's annual total C emissions (Energy Information Association, 2010), if released all in 1 year. Determining the timing and extent of actual C emissions due from tree death depends on a complex set of factors that influence decomposition rates, including temperature, wood density, wood moisture content, and tree diameter (Mackensen *et al.*, 2003), which have not been quantified for these aspen forests. However, most of the C in coarse woody debris is typically respired into the atmosphere during decomposition, and aspen logs have been found to decompose more rapidly than many other boreal tree species with an annual mass loss of 6–8% per year, which suggests that much of the C is likely to be emitted into the atmosphere rather than entering soil matter (Alban & Pastor, 1993; Mackensen *et al.*, 2003; Brais *et al.*, 2006; Michaelian *et al.*, 2011).

Impacts of SAD on regional C stock

Live biomass (and C) loss may be the most important index to assess the impact of drought-induced tree mortality on the ecosystem. It directly affects regional C budgets not only the storage but fluxes (Phillips *et al.*, 2009). After tree dieback, the newly formed dead AGB generally remains in standing dead trees or in fallen coarse woody debris, potentially taking many years to release the C back to atmosphere (see above). High tree mortality can accumulate ground and ladder fuel gradually through a complex process that could potentially trigger high severity ground fires and convert the C sink to a source regionally (Allen, 2007). In addition, tree dieback events would significantly retard the productivity of forest ecosystems, and it could take several decades to recover (via the recruitment of seedlings/saplings and growth of surviving trees) to the predieback condition (Kurz *et al.*, 2008). Although future research will be needed to examine the recovery of these forests and thus C trajectories, preliminary evidence suggests little aspen regrowth or regrowth of other species in SAD areas, which implies that recovery of productivity and C stores could take several decades or more (Worrall *et al.*, 2008, 2010).

Surprisingly, AGB loss from tree dieback has been little studied. To our knowledge, only a few scientific studies measured and/or reported tree dieback induced biomass loss in North America (see Table 3 for summary) and other regions of the world (e.g., Phillips *et al.*, 2009) from drought. Our results suggest that aspen forests in the SJNF might suffer among the most severe biomass loss by recent drought-induced tree mortality in North America across different vegetation types (e.g., Fig. 5b). Magnitude of mean aspen live AGB loss (Mg ha^{-1}) of the study site is 134–422% (depending on the measurements) greater than those estimated in central Canada. In addition, a larger proportion (21.4%) of areas in SJNF experienced high canopy dieback ($\geq 55\%$) than those in the Canadian boreal forests (3%) estimated by the spatial interpolations (Michaelian *et al.*, 2011). Impacts of tree dieback on ecosystem C budgets are pronounced not only inter-regionally but among species as well. Within the same region (southwest Colorado), remote sensing estimates depict greater (202% more) mean live AGB loss in aspen forests than pinyon-juniper (*Pinus edulis–Juniperus osteosperma*) woodlands/forests at lower elevation (Huang *et al.*, 2010). Field surveys also revealed that mean aspen live AGB loss is much higher (180% more) than the mean loss in pinyon-juniper woodlands of the same region (Floyd *et al.*, 2009) and in lodgepole pine forests (78% more) in central Idaho (Pfeifer *et al.*, 2011).

Spatial patterns of drought-induced AGB loss

The consecutive-year drought in the early 2000s was not unique for the region in terms of the low precipitation. However, dry conditions in concert with elevated temperature induced tremendous stress to tree physiology and likely increased vulnerability to insect attack and disease outbreak (Shaw *et al.*, 2005). Physiological mechanisms of drought-induced tree mortality are complicated (McDowell *et al.*, 2008; Adams *et al.*, 2009) and currently being examined for SAD (Anderegg *et al.*, in press), but understanding the influences of temperature and water stress on tree physiology during drought is particularly important because such variables might shed the light on predicting the spatial patterns of tree dieback in western North America (Allen *et al.*, 2010; Overpeck & Udall, 2010). Thus, our remote sensing results, which provide relatively high resolution of spatial patterns of mortality where field measurements would be difficult, could be useful in validating, testing, and informing physiological research into drought-induced dieback. The observed patchy pattern (e.g., Fig. 1a) of tree mortality could imply complex interactions between topographic, micro-climatic, edaphic, insect/pathogen, and even genotype (clonal) effects on spatial patterns.

Worrall *et al.* (2008) investigated the spatial pattern of SAD in four national forests (including SJNF) in southwest Colorado using the USFS Forest Health Aerial Survey data (e.g., Fig. 5c), and they found that SAD patches can be frequently observed at slightly lower elevations (e.g., mean elevation for healthy stands = 2819 m, SAD sites = 2698 m in SJNF), flatter terrain,

and southern to western facing slopes. Our recent field observations and remote sensing estimates revealed that the mortality might have expanded up-slope in recent years, which would suppress an elevation gradient and amplify the variation (Table 2). Our regional scale topographical analysis revealed little relationship between elevation and tree mortality. Additional field observations may be needed at higher elevation (e.g., >2900 m) to validate the potential elevational expansion of aspen dieback. In terms of the influences of slope on tree mortality, Worrall *et al.* (2008) hypothesized that soil moisture is higher in flat benches and bottom slopes during normal years. Hence, rooting is relatively shallow and clones are thus more susceptible to harsh conditions on these settings during the drought. However, our finding did not support this hypothesis, but pronounced variation (SD) may obscure any substantial differences due to slope. Also, this might reflect the discrepancy of using different types of spatial analyses (GIS vs. remote sensing).

Topographic aspect has direct and indirect influences on solar radiation, surface temperature, evaporation, soil moisture, and precipitation of an area. Field ecologists have long recognized that in north-facing aspects would generate wetter and cooler micro-climate locally in the northern hemisphere (Whittaker, 1956, 1960). In contrast, south-facing aspects form harsh environments for plant communities with drier and hotter climate (Haase, 1970). The effect of this prevailing topographic factor is also clearly revealed in this study, which had pronounced influence to the spatial pattern of tree dieback in aspen forests. Note that tree mortality on southwest facing slopes (usually the warmest and driest in the northern hemisphere) was not exceptionally high compared with other south-facing slopes (Table 2). This might imply that environmental dryness to azimuths may vary locally (e.g., wet microsites, Strand *et al.*, 2009a) in this mountainous region.

Feasibility of remote sensing

Satellite remote sensing provides a means of rapid and systematic monitoring of land surfaces at a broad spatial scale. The spatial extent of a Landsat image is relatively large (185 km) with fine spatial resolution (30 m). Therefore, it could be possible to map aspen live AGB loss at the subcontinental scale (e.g., the entire Southwest) with sufficient ground data. In addition, Landsat images can be freely obtained, which allow researchers with limited budget to conduct a similar study. However, it is a challenge to delineate three-dimensional (3D) tree structure variables such as AGB using 2D optical remotely sensed data, and omitting

the information of height (third dimension) could result in significant estimate bias (Huang *et al.*, 2009). Validity of using projected green canopy cover to estimate AGB may be hampered by the structures of trees (Jenkins *et al.*, 2003); it could be even more challenging to use projected NPV cover to project live AGB losses. The results show that although a significant linear relationship was found between live AGB and NPV, there was relatively high variability especially for plots of high AGB losses (Fig. 4a). In some extreme cases, two sites can have apparent difference in live AGB losses but with very similar NPV cover. Therefore, one must take these aforementioned caveats into account when carrying out the research and interpreting results.

Potential for future research

Regional estimates of recent live AGB loss in aspen forests provide a means of understanding the impacts of recent drought on terrestrial C budget and spatial patterns of dieback. Knowledge gained from this study along with long-term frequent field observations may facilitate several promising research directions. Green canopy cover (PV) in severely damaged sites should be mainly contributed from understory shrubs (e.g., mountain snowberry) (Fig. 1b). Therefore, by combining the live AGB loss map (Fig. 5a) with PV cover derived from AutoMCU may help illuminate the effects of SAD on understory plants and shed light on potential changes in whole ecosystem C balance. Also, monitoring severely damaged sites using systematically collected Landsat summer growing season images and field data in the future could facilitate examining the potential for regrowth and regeneration following SAD, which will give a better understanding and provide crucial insight into the long-term fate of C storage in these systems. In addition, estimates of belowground biomass (BGB) loss, especially, are almost entirely absent from studies of mapping C loss due to drought. An aspen clone is well known for its substantial amount belowground C storage, making it one of the largest organisms of the world (Mitton & Grant, 1996). Hence, damages of the tree mortality on total C storage could be substantially larger than just AGB loss, and future research could analyze both the amount of BGB loss due to drought and the fate of that C (e.g., what fraction passes into soil organic matter vs. respiration to the atmosphere). Integrating the remote sensing presented here and modeling (live AGB vs. BGB loss correlations across topoedaphic gradients, root mass decay, etc.) techniques could help us draw a clearer picture of the ramifications of SAD on belowground C budgets. Improved understanding of the over- and understory responses, ecosystem turnover rate, and

BGB dynamics following drought-induced forest mortality all hold potential to increase understanding of C budgets in this widespread vegetation type in North America.

This study demonstrates a straight-forward, integrated synoptic sensing approach to map SAD-induced live AGB losses regionally that requires relatively few field samples and an image acquired in a single growing season. Massive tree mortality events likely generate a substantial amount of NPV cover regardless of vegetation types. Therefore, with the further investigation of the relationship between NPV and live AGB loss across biomes, and the availability of field data (e.g., via a worldwide forest mortality monitoring network), it might be possible to frequently assess the impacts of recent global-change-type drought-induced tree mortality on C dynamics at the continental and global scales and be a potentially effective approach for filling a critical research and monitoring gap (Allen *et al.*, 2010). Establishment of a systematic protocol and monitoring would greatly facilitate planning and management of terrestrial C budgets in response to future climate changes.

References

ACORN (2008) *ACORN 6 User's Manual*. ImSpec LLC, Palmdale, California.

Adams JB, Smith MO, Gillespie AR (1993) Imaging spectroscopy: interpretation based on spectral mixture analysis. In: *Remote Geochemical Analysis: Elemental and Mineralogical Composition* (eds Pieters CM, Englert PA), pp. 145–166. Cambridge University Press, New York.

Adams HD, Guardiola-Claramonte M, Barron-Gafford GA *et al.* (2009) Temperature sensitivity of drought-induced tree mortality portends increased regional die-off under global-change-type drought. *Proceedings of the National Academy of Sciences USA*, **106**, 7063–7066.

Alban DH, Pastor J (1993) Decomposition of aspen, spruce, and pine boles on two sites in Minnesota. *Canadian Journal of Forest Research*, **23**, 1744–1749.

Allen C (2007) Interactions across spatial scales among forest dieback, fire, and erosion in northern New Mexico landscapes. *Ecosystems*, **10**, 797–808.

Allen CD, Macalady AK, Chenchouni H *et al.* (2010) A global overview of drought and heat-induced tree mortality reveals emerging climate change risks for forests. *Forest Ecology and Management*, **259**, 660–684.

Anderegg WRL, Berry JA, Smith DD, Sperry JS, Anderegg LDL, Field CB (in press) Widespread aspen forest die-off: tests of water stress and carbon starvation hypotheses. *Proceedings of the National Academy of Sciences USA*.

Anderson RG, Canadell JG, Randerson JT *et al.* (2011) Biophysical considerations in forestry for climate protection. *Frontiers in Ecology and the Environment*, **9**, 174–182.

Asner GP, Heidebrecht KB (2002) Spectral unmixing of vegetation, soil and dry carbon cover in arid regions: comparing multispectral and hyperspectral observations. *International Journal of Remote Sensing*, **23**, 3939–3958.

Asner GP, Lobell DB (2000) A biogeophysical approach for automated SWIR unmixing of soils and vegetation. *Remote Sensing of Environment*, **74**, 99–112.

Asner GP, Privette JL, Wessman CA, Bateson CA (2000) Impact of tissue, canopy, and landscape factors on the hyperspectral reflectance variability of arid ecosystems. *Remote Sensing of Environment*, **74**, 69–84.

Asner GP, Archer S, Hughes FR, Ansley JR, Wessman CA (2003) Net changes in regional woody vegetation cover and carbon storage in Texas drylands, 1937-1999. *Global Change Biology*, **9**, 316–335.

Barr AG, Black TA, Hogg EH *et al.* (2007) Climatic controls on the carbon and water balances of a boreal aspen forest, 1994-2003. *Global Change Biology*, **13**, 561–576.

Bartos DL, Campbell RB Jr (1998) Decline of quaking aspen in the Interior West: examples from Utah. *Rangelands*, **20**, 17–24.

Bateson AC, Asner GP, Wessman CA (2000) Endmember bundles: a new approach to incorporating endmember variability into spectral mixture analysis. *IEEE Transactions on Geoscience and Remote Sensing*, **38**, 1083–1094.

Brais S, Pare' D, Lierman C (2006) Tree bole mineralization rates of four species of the Canadian eastern boreal forest: implications for nutrient dynamics following stand-replacing disturbances. *Canadian Journal of Forest Research*, **36**, 2331–2340.

Breshears DD, Cobb NS, Rich PM *et al.* (2005) Regional vegetation die-off in response to global-change-type drought. *Proceedings of the National Academy of Sciences USA*, **102**, 15144–15148.

Chambers JQ, Fisher JI, Zeng HC, Chapman EL, Baker DB, Hurtt GC (2007) Hurricane Katrina's carbon footprint on U.S. Gulf Coast Forests. *Science*, **318**, 1107.

Curtis PS, Hanson PJ, Bolstad P, Barford C, Randolph JC, Schmid HP, Wilson KB (2002) Biometric and eddy-covariance based estimates of annual carbon storage in five eastern North American deciduous forests. *Agricultural and Forest Meteorology*, **113**, 3–19.

Daly C, Neilson RP, Phillips DL (1994) A statistical-topographic model for mapping climatological precipitation over mountainous terrain. *Journal of Applied Meteorology*, **33**, 140–158.

Elliot GP, Baker WL (2004) Quaking aspen (*Populus tremuloides*) at treeline: a century of change in the San Juan Mountains, Colorado USA. *Journal of Biogeography*, **31**, 733–745.

Energy Information Association (2010) State Energy Data Release Available at: http://www.eia.gov/state/state-energy-profiles.cfm?sid=CO (accessed 26 April 2011).

Floyd ML, Clifford M, Cobb NS, Hanna D, Delph R, Ford P, Turner D (2009) Relationship of stand characteristics to drought-induced mortality in three Southwestern piñon–juniper woodlands. *Ecological Applications*, **19**, 1223–1230.

Fortin MJ, Dale MRT (2005) *Spatial Analysis: A Guide for Ecologists*. Cambridge University Press, Cambridge.

Fortin MJ, Drapeau P, Legendre P (1989) Spatial autocorrelation and sampling design in plant ecology. *Plant Ecology*, **83**, 209–222.

Gower ST, Vogel JG, Norman JM, Kucharik CJ, Steele SJ, Stow TK (1997) Carbon distribution and aboveground net primary production in aspen, jack pine, and black spruce stands in Saskatchewan and Manitoba, Canada. *Journal of Geophysical Research*, **102**, 29029–29041.

Haase EF (1970) Environmental fluctuations on south-facing slopes in the Santa Catalina Mountains of Arizona. *Ecology*, **51**, 959–974.

Huang C, Marsh SE, McClaran M, Archer S (2007) Postfire stand structure in a semi-arid savanna: cross-scale challenges estimating biomass. *Ecological Applications*, **17**, 1899–1910.

Huang C, Asner GP, Martin R, Barger N, Neff J (2009) Multiscale analysis of tree cover and aboveground carbon stocks in pinyon-juniper woodlands. *Ecological Applications*, **19**, 668–681.

Huang C, Asner GP, Barger N, Neff J, Floyd-Hanna L (2010) Regional carbon losses due to drought-induced tree dieback in piñon-juniper ecosystems. *Remote Sensing of Environment*, **114**, 1471–1479.

Jenkins JC, Chojnacky DC, Heath LS, Birdsey RA (2003) National-scale biomass estimators for United States tree species. *Forest Science*, **49**, 12–35.

Kaakinen S, Kostiainen K, Ek F *et al.* (2004) Stem wood properties of *Populus tremuloides*, *Betula papyrifera* and *Acer saccharum* saplings after 3 years of treatments to elevated carbon dioxide and ozone. *Global Change Biology*, **10**, 1513–1525.

Keen RA (1996) Weather and climate. In: *The Western San Juan Mountains: Their Geology, Ecology, and Human History* (ed Blair R), pp. 113–126. University of Colorado Press, Boulder, Colorado.

Kurz WA, Dymond CC, Stinson G *et al.* (2008) Mountain pine beetle and forest carbon feedback to climate change. *Nature*, **452**, 987–990.

Lowry J, Ramsey RD, Thomas K *et al.* (2007) Mapping moderate-scale land-cover over very large geographic areas within a collaborative framework: a case study of the Southwest Regional Gap Analysis Project (SWReGAP). *Remote Sensing of Environment*, **108**, 59–73.

Mackensen J, Bauhus J, Webber E (2003) Decomposition rates of coarse woody debris - a review with particular emphasis on Australian tree species. *Australian Journal of Botany*, **51**, 27–37.

van Mantgem PJ, Stephenson NL, Byrne JC *et al.* (2009) Widespread increase of tree mortality rates in the Western United States. *Science*, **323**, 521–524.

Marchetti SB, Worrall JJ, Eager T (in press) Secondary insects and diseases contribute to sudden aspen decline in southwestern Colorado, USA. *Canadian Journal of Forest Research*.

McDowell N, Pockman WT, Allen CD *et al.* (2008) Mechanisms of plant survival and mortality during drought: Why do some plants survive while others succumb to drought? *New Phytologist*, **178**, 719–739.

Michaelian M, Hogg EH, Hall RJ, Arsenault E (2011) Massive mortality of aspen following severe drought along the southern edge of the Canadian boreal forest. *Global Change Biology*, **17**, 2084–2094.

Mitton JB, Grant MC (1996) Genetic variation and the natural history of quaking aspen. *BioScience*, **46**, 25–31.

Moran PAP (1950) Notes on continuous stochastic phenomena. *Biometrika*, **37**, 17–23.

Overpeck J, Udall B (2010) Dry times ahead. *Science*, **328**, 1642–1643.

Pastor J, Aber JD, Melillo JM (1984) Biomass prediction using generalized allometric regressions for some northeast tree species. *Forest Ecology and Management*, **7**, 265–274.

Perala DA (1990) *Populus tremuloides*. In: *Silvics of North America. Hardwoods* (eds Burns RM, Honkala BH), pp. 555–569. United States Department of Agriculture Forest Service, Washington, DC, USA.

Pfeifer EM, Hicke JA, Meddens AJH (2011) Observations and modeling of aboveground tree carbon stocks and fluxes following a bark beetle outbreak in the western United States. *Global Change Biology*, **7**, 339–350.

Phillips OL, Aragão LEOC, Lewis SL *et al.* (2009) Drought sensitivity of the Amazon rainforest. *Science*, **323**, 1344–1347.

Rehfeldt GE, Ferguson DE, Crookston NL (2009) Aspen, climate, and sudden decline in western USA. *Forest Ecology and Management*, **258**, 2353–2364.

Royer PD, Cobb NS, Clifford MJ, Huang C, Breshears DD, Adams HD, Villegas JC (2011) Extreme climatic event-triggered overstorey vegetation loss increases understorey solar input regionally: primary and secondary ecological implications. *Journal of Ecology*, **99**, 714–723.

Shaw JD, Steed BE, DeBlander LT (2005) Forest Inventory and Analysis (FIA) annual inventory answers the question: What is happening to pinyon-juniper woodlands? *Journal of Forestry*, **103**, 280–285.

Shepperd WD, Bartos DL, Mata SA (2001) Above- and below-ground effects of aspen clonal regeneration and succession to conifers. *Canadian Journal of Forest Research*, **31**, 739–745.

Strand EK, Vierling LA, Bunting SC, Gessler PE (2009a) Quantifying successional rates in western aspen woodlands: current conditions, future predictions. *Forest Ecology and Management*, **257**, 1705–1715.

Strand EK, Vierling LA, Bunting SC (2009b) A spatially explicit model to predict future landscape composition of aspen woodlands under various management scenarios. *Ecological Modelling*, **220**, 175–191.

Whittaker RH (1956) Vegetation of the Great Smoky Mountains. *Ecological Monographs*, **26**, 1–80.

Whittaker RH (1960) Vegetation of the Siskiyou Mountains, Oregon and California. *Ecological Monographs*, **30**, 279–338.

Worrall JJ, Egeland L, Eager T, Mask RA, Johnson EW, Kemp PA, Shepperd WD (2008) Rapid mortality of *Populus tremuloides* in southwestern Colorado, USA. *Forest Ecology and Management*, **255**, 686–696.

Worrall JJ, Marchetti SB, Egeland L, Mask RA, Eager T, Howell B (2010) Effects and etiology of sudden aspen decline in southwestern Colorado, USA. *Forest Ecology and Management*, **260**, 638–648.